

Paper 63-2 has been designated as a Distinguished Paper at Display Week 2018. The full-length version of this paper appears in a Special Section of the *Journal of the Society for Information Display (JSID)* devoted to Display Week 2018 Distinguished Papers. This Special Section will be freely accessible until December 31, 2018 via:

http://onlinelibrary.wiley.com/page/journal/19383657/homepage/display_week_2018.htm

Authors that wish to refer to this work are advised to cite the full-length version by referring to its DOI:

<https://doi.org/10.1002/jsid.652>

Dependency of Speckle Reduction by Wavelength Diversity on Angular Diversity in Laser Projection System

Hirota Yamada¹, Kengo Moriyasu², Hiroto Sato¹, Hidekazu Hatanaka³

¹Ushio Inc., Hyogo, Japan

²Ushio Opto Semiconductors, Inc., Kyoto, Japan

³Ushio Inc., Tokyo, Japan

Abstract

In laser projection system, speckle reduction by wavelength and angular diversities are often treated independently. Here, it is experimentally shown that there is a clear dependency between wavelength and angular diversities. Also, speckle reduction by wavelength and angular diversities are theoretically investigated. The theoretical calculation agrees well the experimental results.

Author Keywords

Speckle; laser projectors; wavelength diversity; angular diversity.

1. Objective and Background

Recently, laser projectors have been rapidly developed. One of the most serious problems of laser projectors is speckle, which seriously deteriorates the image quality.

The most commonly used and effective methods to reduce speckle include wavelength diversity, polarization diversity, angular diversity, and temporal averaging of speckle (temporal diversity) using moving or vibrating diffuser. In the laser projection systems, combinations of some or all of these methods are used to suppress speckle to the acceptable level.

As shown by Goodman [1], angular diversity and temporal diversity are not independent; in order to reduce speckle down to the value limited by angular diversity, temporal diversity needs to be large enough. On the other hand, wavelength diversity and angular diversity are treated independently in many cases [2,3]. However, in Ref. [4], the authors showed that wavelength diversity is dependent on angular diversity, as well as incidence and observation angles in laser projection systems. In this paper, the theoretical model to express the dependency of wavelength and angular diversity is derived. The experimental results are compared with the theoretical calculation.

2. Theoretical model

(a) Speckle contrast with different wavelengths and angles: In many laser projection systems, all of wavelength diversity, angular diversity (including temporal diversity), and polarization diversity are used to reduce speckle. As shown in Ref. [4], speckle reduction by angular diversity and wavelength diversity are not independent. Thus, the speckle contrast is written as:

$$C = C_{\lambda, \Omega} C_{\sigma}, \quad (1)$$

where $C_{\lambda, \Omega}$ is the speckle reduction factor by wavelength diversity and angular diversity together. In this section, the mathematical form of $C_{\lambda, \Omega}$ is derived.

In order to derive the speckle contrast with wavelength diversity and angular diversity, the following assumptions are made:

(1) Any components of the incident light on screen with different incident angles are mutually incoherent, that is, light from any two points on the exit pupil of projection lens are incoherent.

(2) Any component of the incident light with incident angle (α, β)

and wavelength λ forms fully developed speckle, which is written as $I(x, y; \lambda, \alpha, \beta)$, where (x, y) are the coordinates on the image plane. $I(x, y; \lambda, \alpha, \beta)$ is normalized to satisfy $\iint dx dy I(x, y; \lambda, \alpha, \beta) = I_0$, which does not depend on λ, α , or β .

(3) Only surface and single scattering occurs on screen.

When the wavelength and angular distribution of the incident light can be written as $f(\lambda, \alpha, \beta)$ which satisfies the normalization condition $\iint d\lambda d\Omega_{\alpha, \beta} f(\lambda, \alpha, \beta) = 1$, the speckle intensity at (x, y) on the image plane can be expressed as:

$$I(x, y) = \iint d\lambda d\Omega_{\alpha, \beta} f(\lambda, \alpha, \beta) I(x, y; \lambda, \alpha, \beta), \quad (2)$$

where $\int d\Omega_{\alpha, \beta}$ expresses the integral over all incident angles. Therefore, the mean intensity and the second moment of the speckle pattern are:

$$\begin{aligned} \langle I \rangle &= \iint dx dy I(x, y) \\ &= \iint d\lambda d\Omega_{\alpha, \beta} f(\lambda, \alpha, \beta) \left(\iint dx dy I(x, y; \lambda, \alpha, \beta) \right) = I_0, \end{aligned} \quad (3)$$

$$\begin{aligned} \langle I^2 \rangle &= \iint dx dy I^2(x, y) \\ &= \iint d\lambda_1 d\Omega_{\alpha_1, \beta_1} \iint d\lambda_2 d\Omega_{\alpha_2, \beta_2} f(\lambda_1, \alpha_1, \beta_1) f(\lambda_2, \alpha_2, \beta_2) \\ &\quad \times \left(\iint dx dy I(x, y; \lambda_1, \alpha_1, \beta_1) I(x, y; \lambda_2, \alpha_2, \beta_2) \right) \\ &= \iint d\lambda_1 d\Omega_{\alpha_1, \beta_1} \iint d\lambda_2 d\Omega_{\alpha_2, \beta_2} \\ &\quad \times f(\lambda_1, \alpha_1, \beta_1) f(\lambda_2, \alpha_2, \beta_2) \Gamma_I(\lambda_1, \alpha_1, \beta_1, \lambda_2, \alpha_2, \beta_2), \end{aligned} \quad (4)$$

where $\Gamma_I(\lambda_1, \alpha_1, \beta_1, \lambda_2, \alpha_2, \beta_2) = \iint dx dy I(x, y; \lambda_1, \alpha_1, \beta_1) \times I(x, y; \lambda_2, \alpha_2, \beta_2)$ is the autocorrelation function of the intensity of the speckle field. According to Ref. [1], the autocorrelation function of the intensity of fully developed speckle pattern is written as:

$$\Gamma_I = I_0^2 \left[1 + |\mu_A(\lambda_1, \alpha_1, \beta_1, \lambda_2, \alpha_2, \beta_2)|^2 \right], \quad (5)$$

where μ_A is the normalized complex correlation function of the amplitude, of which form is discussed in the next subsection. Thus, the speckle contrast is written as:

$$\begin{aligned} C_{\lambda, \Omega} &= \frac{\sqrt{\langle I^2 \rangle - \langle I \rangle^2}}{\langle I \rangle} \\ &= \sqrt{\iint d\lambda_1 d\Omega_{\alpha_1, \beta_1} \iint d\lambda_2 d\Omega_{\alpha_2, \beta_2} f(\lambda_1, \alpha_1, \beta_1) f(\lambda_2, \alpha_2, \beta_2) |\mu_A|^2}. \end{aligned} \quad (6)$$

(b) Normalized complex correlation function of the amplitude:

In Ref. [5], McKechnie derived the expression of the normalized correlation function of the amplitude. As shown in Fig. 1, let the coordinates on screen plane and image plane be (ξ, η) and (x, y) ,

respectively. When the ξ - and η -components of the directional cosines of the wave vector of incident light are (α_i, β_i) and those of the observation light are (α_o, β_o) , the amplitude of the field of the scattered light on the rough surface of screen is given by:

$$a(\xi, \eta) = E_0 \exp \left(i\Phi(\xi, \eta) + \frac{2\pi i}{\lambda} \{(\alpha_i \xi + \beta_i \eta) - (\alpha_o \xi + \beta_o \eta)\} \right), \quad (7)$$

where Φ is the phase distribution imposed on the scattered light due to random surface profile of screen, and E_0 is a constant. It is assumed that the screen is illuminated uniformly. If the incident light scattered on the surface of screen and only single scattering occurs, Φ is written as:

$$\Phi(\xi, \eta) = q_z h(\xi, \eta), \quad (8)$$

where q_z is the vertical component of the scattering vector on screen and $h(\xi, \eta)$ is the surface height profile of screen. The amplitude of the speckle field on the image plane $A(x, y)$ is then written in terms of the point spread function of optical system, $k(\lambda; x, y, \xi, \eta)$, as follows:

$$A(x, y) = \iint d\xi d\eta k(x, y; \xi, \eta) a(\xi, \eta). \quad (9)$$

Next, let Γ_A be the correlation function of the amplitude of speckle fields with wavelength and incident angles $(\lambda_1, \alpha_{i1}, \beta_{i1})$ and $(\lambda_2, \alpha_{i2}, \beta_{i2})$, and the same observation angle (α_o, β_o) . Γ_A is written as:

$$\begin{aligned} \Gamma_A(x_1, y_1, x_2, y_2) &= \overline{A_1(x_1, y_1) A_2^*(x_2, y_2)} \\ &= \iint d\xi_1 d\eta_1 \iint d\xi_2 d\eta_2 \left\{ k(x_1, y_1; \xi_1, \eta_1) k^*(x_2, y_2; \xi_2, \eta_2) \right. \\ &\quad \left. \times \overline{a_1(\xi_1, \eta_1) a_2^*(\xi_2, \eta_2)} \right\}, \end{aligned} \quad (10)$$

where overlines express the statistical average.

As shown in Ref. [1], we assume that the surface height distribution of the screen is Gaussian distribution with the standard deviation of σ_h and that the correlation width of the scattered field is small enough to be treated as the delta function. The statistical average of the product of the scattered light fields is written as:

$$\begin{aligned} &\overline{a_1(\xi_1, \eta_1) a_2^*(\xi_2, \eta_2)} \\ &= M_h(\Delta q_z) \\ &\times \exp \left[2\pi i \frac{(\alpha_{i1} - \alpha_o) \xi_1 + (\beta_{i1} - \beta_o) \eta_1}{\lambda_1} \right] \\ &\times \exp \left[-2\pi i \frac{(\alpha_{i2} - \alpha_o) \xi_2 + (\beta_{i2} - \beta_o) \eta_2}{\lambda_2} \right] \\ &\times \delta(\xi_1 - \xi_2) \delta(\eta_1 - \eta_2), \end{aligned} \quad (11)$$

where the insignificant constant term was omitted,

$$M_h(\Delta q_z) = \exp \left(-\frac{1}{2} \sigma_h^2 (\Delta q_z)^2 \right), \quad (12)$$

and $\Delta q_z = q_{z1} - q_{z2}$ is the difference of the vertical components of the scattering vectors.

Let $P(u, v)$ be the pupil function of the imaging optics and M be the magnification of the imaging system. The point spread

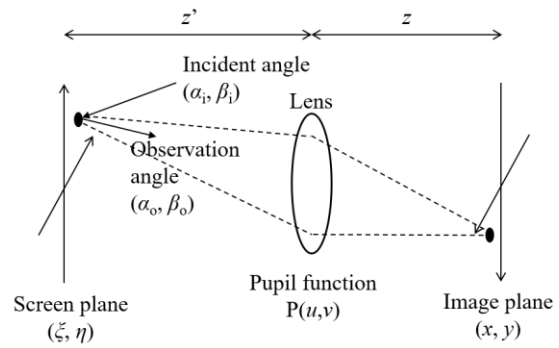


Figure 1. Schematic diagram of imaging system.

function can be written as [6]:

$$k(\lambda; x, y, \xi, \eta) = \frac{1}{\lambda^2 z z'} \iint du dv P(u, v) e^{-i \frac{2\pi}{\lambda z} \{(x - M\xi)u + (y - M\eta)v\}}, \quad (13)$$

where z' is the distance from the screen to the imaging optics, z is the distance from the imaging optics to the image plane as shown in Fig. 1, and z and z' satisfy $M = z/z'$. Substituting Eqs. (11) and (13) to Eq. (10) and omitting insignificant phase terms, the correlation function is obtained as:

$$\begin{aligned} \Gamma_A &= \frac{1}{z^2} M_h(\Delta q_z) \\ &\times \iint du_0 dv_0 P(\lambda_1 u_0 - z'(\alpha_{i1} - \alpha_o), \lambda_1 v_0 - z'(\beta_{i1} - \beta_o)) \\ &\quad \times P^*(\lambda_2 u_0 - z'(\alpha_{i2} - \alpha_o), \lambda_2 v_0 - z'(\beta_{i2} - \beta_o)) \\ &\quad \times \exp \left(2\pi i \left\{ \frac{u_0(x_2 - x_1)}{z} + \frac{v_0(y_2 - y_1)}{z} \right\} \right). \end{aligned} \quad (14)$$

where the following changes of variables were performed: $u = \lambda_1 u_0 - z'(\alpha_{i1} - \alpha_o)$, and $v = \lambda_1 v_0 - z'(\beta_{i1} - \beta_o)$. Putting $x_1 = x_2$, $y_1 = y_2$, the normalized correlation function of the amplitude is:

$$\begin{aligned} &\mu_A(\lambda_1, \alpha_{i1}, \beta_{i1}, \lambda_2, \alpha_{i2}, \beta_{i2}) \\ &= \frac{\Gamma_A}{\Gamma_A(\lambda_1 = \lambda_2, \alpha_{i1} = \alpha_{i2}, \beta_{i1} = \beta_{i2})} \\ &= M_h(\Delta q_z) \Psi(\lambda_1, \alpha_{i1}, \beta_{i1}, \lambda_2, \alpha_{i2}, \beta_{i2}; \alpha_o, \beta_o), \end{aligned} \quad (15)$$

where

$$\begin{aligned} &\Psi(\lambda_1, \alpha_{i1}, \beta_{i1}, \lambda_2, \alpha_{i2}, \beta_{i2}; \alpha_o, \beta_o) \\ &= \iint du_0 dv_0 P(\lambda_1 u_0 - z'(\alpha_{i1} - \alpha_o), \lambda_1 v_0 - z'(\beta_{i1} - \beta_o)) \\ &\quad \times P^*(\lambda_2 u_0 - z'(\alpha_{i2} - \alpha_o), \lambda_2 v_0 - z'(\beta_{i2} - \beta_o)) \\ &\quad \div \left[\iint du_0 dv_0 [P(\lambda_1 u_0, \lambda_1 v_0)]^2 \iint du_0 dv_0 [P(\lambda_2 u_0, \lambda_2 v_0)]^2 \right]^{\frac{1}{2}}. \end{aligned} \quad (16)$$

When the imaging system consists of an aberration free circular lens with the radius of r , the pupil function is described as:

$$P(u, v) = \begin{cases} 1 & (u^2 + v^2 \leq r^2) \\ 0 & (u^2 + v^2 > r^2) \end{cases}. \quad (17)$$

Substituting Eq. (17) to Eq. (16), Ψ can be written as:

$$\Psi = \frac{S}{\sqrt{S_1 S_2}}, \quad (18)$$

where S_1 and S_2 are the area of the following two circles, and S is the overlapped area of the following two circles:

- Circle 1: radius r/λ_1 , center $(z'(\alpha_{i1}-\alpha_o)/\lambda_1, z'(\beta_{i1}-\beta_o)/\lambda_1)$,
- Circle 2: radius r/λ_2 , center $(z'(\alpha_{i2}-\alpha_o)/\lambda_2, z'(\beta_{i2}-\beta_o)/\lambda_2)$.

(c) Speckle contrast of two wavelength lasers with the same angular distribution: Assuming that incident light consists of two wavelength components of which linewidth can be approximated as the delta function, and that the angular distribution of the incident light is a top-hat distribution with half angle divergence of θ_{div} and the center angle of $(\alpha_i, 0)$, the distribution function of the incident light can be approximated as:

$$f(\lambda, \alpha, \beta) \approx \begin{cases} B \frac{\delta(\lambda - \lambda_1) + \delta(\lambda - \lambda_2)}{2} & ((\alpha - \alpha_i)^2 + \beta^2 < \theta_{div}^2) \\ 0 & (\text{otherwise}) \end{cases} \quad (19)$$

where B is a normalization constant. Substituting Eqs. (15) and (19) to Eq. (6), the speckle contrast is obtained as follows:

$$C_{\lambda, \Omega} \approx \left(\left(\frac{B}{2} \right)^2 \int_{(\alpha_1 - \alpha_i)^2 + \beta_1^2 < \theta_{div}^2} d\Omega_{\alpha_1, \beta_1} \int_{(\alpha_2 - \alpha_i)^2 + \beta_2^2 < \theta_{div}^2} d\Omega_{\alpha_2, \beta_2} \times \sum_{i, j \in \{1, 2\}} |M_h(\Delta q_z) \Psi(\lambda_i, \alpha_1, \beta_1, \lambda_j, \alpha_2, \beta_2)|^2 \right)^{1/2} \quad (20)$$

3. Experimental method

The frequency doubled Ncnel green lasers (530-550 nm) were used for the speckle measurement. An experimental setup is shown in Fig. 2. Light from one laser or two lasers with different wavelengths entered a bundle fiber. The emitted light from the fiber was diffused by a vibrating diffuser and then converged into a second optical fiber connected with a hexagonal rod integrator. The edge image of the rod integrator was projected onto a screen using a collimation lens and a condenser lens. The collimation lens was chosen from three lenses with different focal lengths to change the angular diversity. A focal length of the condenser lens was fixed to 750 mm. A silver screen with gain 2.4 was used.

The resulting speckle pattern was then measured using a cooled CCD camera. A focal length of the objective lens of the CCD camera was 50 mm, and a circular aperture was mounted in front of the camera. Both the center angles of the incidence direction and observation direction have only ξ -components, α_i and α_o ; the η -components are zero ($\beta_i = \beta_o = 0$). The detailed description of the experimental setup can be found in Ref. [4].

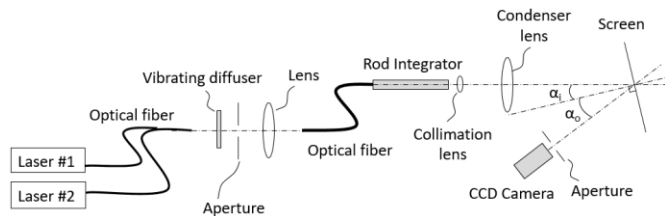


Figure 2. Schematic diagram of an experimental setup.

4. Results

(a) Speckle reduction by angular diversity with one wavelength laser: First, the speckle contrast of one laser with various angular diversity was measured on the silver screen. The results were compared with the theoretical calculation.

The incidence and observation angles were 0° and 17° , respectively. The focal length of the collimation lens was $f = 7.86$ mm. In Ref. [1], Goodman shows that the speckle contrast with angular diversity can be approximated as $C_\Omega \approx (\Omega_d / \Omega_p)^{1/2}$, where Ω_p is the solid angle subtended by the projector lens, and $\Omega_d \propto (D/L)^2$ is the solid angle subtended by the camera aperture, where D is the aperture diameter in front of the camera, and L is the camera-to-screen distance. Therefore, the angular diversity can be changed by changing D and L . D was changed from 0.2 mm to 2.0 mm and L was changed from 240 mm to 700 mm in the experiment.

The measured speckle contrasts were shown in Fig. 3. Since Ω_d is proportional to $(D/L)^2$, the speckle contrast is expected to be approximately proportional to D/L . However, as shown in Fig. 3, the speckle contrast is not proportional to D/L when D/L is large, which means that this approximation is not good when angular diversity is small.

The red line in Fig. 3 shows the root sum square C_{total} of the calculated speckle contrast C_{calc} and the non-speckle contrast $C_{non-speckle}$ due to non-speckle pattern as follows:

$$C_{total} = (C_{calc}^2 + C_{non-speckle}^2)^{1/2}. \quad (21)$$

The value of $C_{non-speckle}$ was chosen to be 6% from the results of two wavelength lasers in the next subsection, and the same value was used throughout all the results in this paper. C_{calc} was calculated by Eq. (20) for $\theta_{div} = 0.0015$ rad, $\sigma_h = 3.2 \mu\text{m}$, $\alpha_i = 0^\circ$, $\alpha_o = 17^\circ$, and $\lambda = (\lambda_1 = \lambda_2) = 550$ nm. θ_{div} was used as a fitting parameter. The value of σ_h depends on screen, but it does not affect the speckle contrast of one wavelength laser. Thus, the value of σ_h was determined from the results in the next subsection. Other parameters, such as incidence and observation angles and the wavelength were taken from the experimental setup.

The angular divergence θ_{div} was chosen to be 0.0015 rad so that the calculated contrast by Eq. (21) agrees with the experimental results. As shown in Fig. 3, the calculated contrasts and the measured speckle contrasts showed a good agreement even when D/L is large. Since the magnification of the imaging lenses to project the edge image of the rod onto the screen is about 200x when the collimation lens with the focal length of 7.86 mm is used, the divergence of the light emitting from the rod is calculated as 0.30 rad in half angle, which is slightly smaller than the NA of the optical fiber (0.39NA).

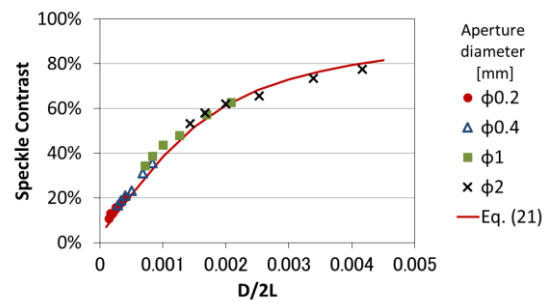


Figure 3. The speckle contrast of one laser with various angular diversity. Red line shows the calculated contrast.

(b) Speckle reduction by angular and wavelength diversities with two wavelength lasers: Next, we measured the speckle contrast of two lasers with various wavelength intervals. The aperture diameter of the camera and the camera-to-screen distance were fixed to 1.0 mm and 700 mm, respectively.

Figure 4 shows the speckle contrast of two lasers divided by the average contrast of each laser when the observation angle was 6° , 17° , 27° , and 45° . The incident angle and the focal length of the collimation lens were fixed to 0° and 7.86 mm, respectively. The speckle contrasts of two lasers were normalized to the average speckle contrast of each laser in order to separate the speckle reduction effect of wavelength diversity from other diversities.

The red, green, blue and black solid lines show the calculated contrasts when the observation angle is 6° , 17° , 27° , and 45° , respectively. Here, $C_{\text{non-speckle}}$ and σ_h were used as fitting parameters. It is expected that when the wavelength interval of two lasers are large enough, the normalized speckle contrast becomes 0.707 ($=1/\sqrt{2}$). However, as shown in Fig. 4, the normalized speckle contrasts are around 0.72-0.73 even when the wavelength interval is large enough. A possible reason is that measured contrasts included a contrast due to non-speckle patterns, such as screen texture. If there is a non-speckle pattern, the total contrast of two lasers does not decrease by a factor of $\sqrt{2}$ even when the wavelength interval of two lasers are large enough. We used the contrast of 6% as the non-speckle contrast $C_{\text{non-speckle}}$ and calculated the total contrast using Eq. (21) so that the normalized contrast of two lasers becomes 0.72 when the

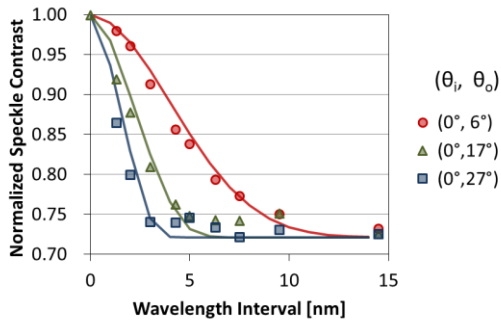


Figure 4. The speckle contrast of two lasers divided by the average speckle contrast of each laser with various observation angles. The focal length of the collimation lens was fixed to 7.86 mm.

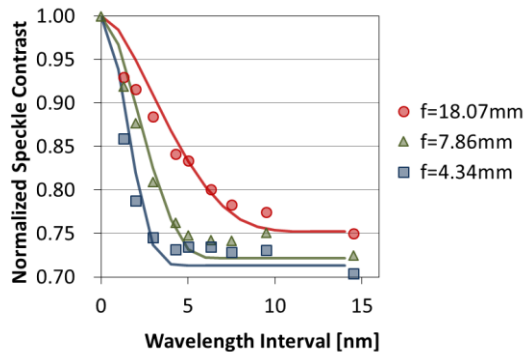


Figure 5. The speckle contrast of two lasers divided by the average speckle contrast of each laser with various focal lengths of the collimation lens. The incidence and observation angles were fixed to $(0^\circ, 17^\circ)$.

wavelength interval is large enough.

σ_h was chosen to be $3.2 \mu\text{m}$ so that the calculated values can reproduce the experimental results. Since θ_{div} depends on the focal length of the collimation lens in our experimental setup, the same value is used for the same collimation lens. Thus, the same angular divergence θ_{div} as the previous subsection, 0.0015 rad, was used. The calculated contrasts were in a good agreement with the experimental results.

Then, speckle contrasts were measured for various angular diversities. The incidence and observation angles were fixed to $(\alpha_i, \alpha_o) = (0^\circ, 17^\circ)$, but the focal length of the collimation lens after the rod integrator was changed. Figure 5 shows the speckle contrast of two lasers divided by the average speckle contrast of each laser with various wavelength intervals and the focal lengths of the collimation lens. The results clearly show that the speckle reduction by wavelength diversity depends on the amount of angular diversity; the more the angular diversity is, the larger the wavelength interval needs to be to have the same amount of speckle reduction by wavelength diversity.

The solid lines are the calculated contrasts in the same way as Fig. 5. The half angle divergence θ_{div} of 0.00085 rad, 0.0015 rad, and 0.0030 rad were used for $f=18.07 \text{ mm}$, $f=7.86 \text{ mm}$, and $f=4.34 \text{ mm}$, respectively. The calculated results successfully reproduced the dependency of the speckle reduction by wavelength diversity on angular diversity.

5. Conclusion

In conclusion, it was shown that speckle reduction by wavelength diversity depends largely on the amount of angular diversity. The larger wavelength interval was needed to reduce speckle when the angular diversity was larger. Also, the speckle reduction by the combination of wavelength and angular diversities was investigated theoretically. The theoretical model successfully expressed the speckle reduction by wavelength and angular diversities together. The speckle contrast calculated from the theoretical equation agreed well with the experimental results.

6. Impact of our research

In this paper, it is shown that the effect of wavelength diversity depends on the degree of angular diversity. The results would be helpful to determine the wavelength selection to suppress speckle effectively in laser projection system depending on individual projection conditions.

7. References

- [1] J. W. Goodman, *Speckle Phenomena in Optics* (Roberts and Company Publishers, 2007).
- [2] J. I. Trisnadi, "Speckle contrast reduction in laser projection displays," *Proc. SPIE* **4657**, 131–137 (2002).
- [3] T.-T.-K. Tran, Ø. Svensen, X. Chen, and M. Nadeem Akram, "Speckle reduction in laser projection displays through angle and wavelength diversity," *Appl. Opt.* **55**, 1267–1274 (2016).
- [4] H. Yamada, K. Moriyasu, H. Sato, and H. Hatanaka, "Effect of incidence/observation angles and angular diversity on speckle reduction by wavelength diversity in laser projection systems," *Opt. Express* **25**, 32132–32141 (2017).
- [5] T. S. McKechnie, "Speckle Reduction," in *Laser Speckle and Related Phenomena*, J. C. Dainty, ed. (Springer-Verlag, 1975).
- [6] J. W. Goodman, *Introduction to Fourier Optics*, Second Ed. (The McGraw-Hill Companies, Inc., 1996).